Eukaryotic *Penelope*-Like Retroelements Encode Hammerhead Ribozyme Motifs

Amelia Cervera[1] and Marcos De la Peña*[,1]

[1]Instituto de Biología Molecular y Celular de Plantas (UPV-CSIC), Valencia, Spain

***Corresponding author:** E-mail: rivero@ibmcp.upv.es.

Associate editor: Csaba Pal

Abstract

Small self-cleaving RNAs, such as the paradigmatic Hammerhead ribozyme (HHR), have been recently found widespread in DNA genomes across all kingdoms of life. In this work, we found that new HHR variants are preserved in the ancient family of *Penelope*-like elements (PLEs), a group of eukaryotic retrotransposons regarded as exceptional for encoding telomerase-like retrotranscriptases and spliceosomal introns. Our bioinformatic analysis revealed not only the presence of minimalist HHRs in the two flanking repeats of PLEs but also their massive and widespread occurrence in metazoan genomes. The architecture of these ribozymes indicates that they may work as dimers, although their low self-cleavage activity in vitro suggests the requirement of other factors in vivo. In plants, however, PLEs show canonical HHRs, whereas fungi and protist PLEs encode ribozyme variants with a stable active conformation as monomers. Overall, our data confirm the connection of self-cleaving RNAs with eukaryotic retroelements and unveil these motifs as a significant fraction of the encoded information in eukaryotic genomes.

Key words: **intron, LTR, retrotransposon, RNA self-cleavage, SINE, telomerase.**

The knowledge of the manifold roles of RNA has transformed our perception of this macromolecule from that of a mere intermediary into a key component of present and past life on Earth. The discovery of ribozymes (Kruger et al. 1982) was a milestone in this change of paradigm, giving strong support for the hypothesis of a prebiotic RNA world (Gilbert 1986). Among the simplest ribozymes, we find a family of six small self-cleaving RNAs (Ferre-D'Amare and Scott 2010; Roth et al. 2014), with the Hammerhead ribozyme (HHR) as the most studied member (Hutchins et al. 1986; Prody et al. 1986). The HHR is made up by three double helixes (I–III) that surround a conserved catalytic core (fig. 1*A*). The motif adopts a γ-shaped fold, where Helix III coaxially stacks with Helix II, and Helix I is positioned in parallel interacting with Helix II through tertiary interactions required for efficient self-cleavage in vivo (De la Peña et al. 2003; Khvorova et al. 2003; Martick and Scott 2006). The HHR was discovered in small RNA plant pathogens, where it catalyzes a transesterification self-cleavage reaction during their rolling-circle replication (Symons 1997). HHRs were also found in DNA genomes of a few unrelated eukaryotes either plants (Daros and Flores 1995; Przybilski et al. 2005) or metazoans (Epstein and Gall 1987; Ferbeyre et al. 1998; Rojas et al. 2000; Martick et al. 2008). In 2010, our lab reported the widespread presence of HHRs from bacterial to eukaryal genomes, including humans (De la Peña and Garcia-Robles 2010a, 2010b). Similar reports confirmed and extended our observations (Jimenez et al. 2011; Perreault et al. 2011; Seehafer et al. 2011), unveiling the HHR as an ubiquitous catalytic RNA in all life kingdoms (Hammann et al. 2012). Eukaryotic HHRs usually occur in small tandem DNA repeats close to retrotransposons and telomeric sequences, suggesting a relationship with retroelements (De la Peña and Garcia-Robles 2010b). Retrotransposons are major constituents of eukaryotic genomes and have been usually divided into two categories: Long terminal repeats (LTR) and non-LTR retrotransposons. There is a third unusual type, the *Penelope*-Like Elements (PLEs), widespread among eukaryotes (Evgen'ev et al. 1997; Evgen'ev and Arkhipova 2005). Genomic PLEs are delimited by two direct repeats (PLTRs) flanking a single open reading frame (ORF) with two domains: A reverse transcriptase (RT) similar to Telomerase RTs, and an endonuclease (EN) with the GIY–YIG motif found in group I intron ENs (fig. 1*C*). PLEs are also remarkable for containing spliceosomal introns, an intriguing feature for a transposon that replicates through RNA intermediates (Arkhipova et al. 2003).

In this work, we report the conserved occurrence of new HHR variants in the PLTRs of all PLE sequences that we found deposited in the databases, adding an extra level of complexity to this ancient family of retroelements.

Results

Defining a New Minimal HHR Motif

Most metazoan HHRs are type-I motifs with a similar architecture (hereafter, canonical HHRs); Helixes I (6 bp) and II (4 bp) interact through conserved loop nucleotides, whereas Helix III usually has a short stem (1–2 bp) capped by a small (2–4 nt) and palindromic loop (fig. 1*A* and supplementary fig. S1, Supplementary Material online). Such an unstable Helix III impedes efficient RNA self-cleavage as a monomeric HHR, but when a second copy of the ribozyme is in the vicinity (i.e., tandem repeats), the two HHRs can fold into an active dimeric ribozyme (fig. 1*A*) (Forster et al. 1988). This

Letter

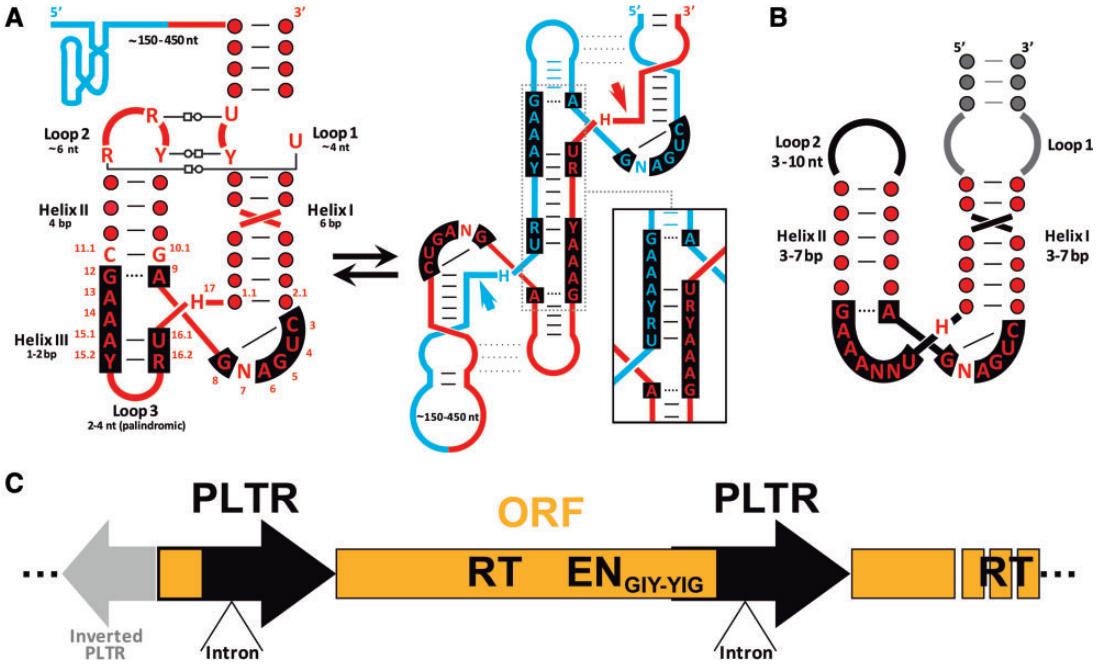

FIG. 1. (*A*) HHR conformations in a tandem repeat, either as monomers (left) or as a dimeric active conformation (right). The monomeric HHR shows the conserved core positions and their numbering (Hertel et al. 1992). The right inset shows an extended Helix III made up with a minimal core. (*B*) Secondary structure of the min-HHR descriptor. Loop 1 and closing stem I not included in the descriptor are shown in gray. (*C*) Schematic representation of a PLE. Flanking repeats are shown as black arrows (PLTRs) and the ORF as an orange rectangle.

arrangement is thought to offer a form of regulation in small RNA pathogens, where self-cleavage would be allowed during synthesis of multimeric forms, but avoided in the monomeric circular RNAs (Flores et al. 2004). Hence, we reasoned that no Helix III/loop 3 should be required in a single HHR, so a minimal HHR motif (min-HHR) with only the conserved nucleotides would be equally capable of adopting a dimeric active conformation (fig. 1*A* inset). A relaxed descriptor for such a min-HHR was defined (fig. 1*B*) and used for bioinformatic searches (see Materials and Methods).

Evolutionary Conservation of min-HHRs in Metazoan PLEs

Initial searches in a set of metazoan genomes resulted in an overwhelming number of min-HHRs, making it difficult to analyze them. Thus, individual genomes were analyzed separately.

The *Schistosoma mansoni* genome (Berriman et al. 2009) is known to contain thousands of canonical HHRs (Ferbeyre et al. 1998; De la Peña and Garcia-Robles 2010a), and our minimal descriptor revealed the presence of approximately 2,000 min-HHRs. The new motifs showed high sequence heterogeneity and were classified into major consensus families with a very similar architecture (fig. 2*A* and supplementary fig. S2, Supplementary Material online): Larger than usual Helix II (7–8 bp), a shorter Helix I (4–5 bp) with a poorly defined loop 1, and an unpaired nucleotide at the 5′-end of stem II similar to the one reported in some canonical HHRs (De la Peña and Flores 2001). In a few cases, HHRs occurred in tandem arrangements separated by approximately 3 kb. Analysis of the flanked sequence revealed a retrotranscriptase ORF of the *Cercyon* family of PLEs (Arkhipova et al. 2013), and more precisely, min-HHRs occurred in their PLTRs. Other examples of dual min-HHRs were also found close to each other (~100–700 bp) but in opposite strands. Thus, most of the motifs were found widespread as single elements and were probably related to truncated PLEs. Homology searches with the *Cercyon* element revealed an interesting HHR variant not considered in our descriptor, which showed a covariation within the catalytic core of the ribozyme (U_3–A_8 instead of C_3–G_8; fig. 2*A* inset). A descriptor with this new core retrieved approximately 1,300 hits that again showed high sequence heterogeneity and mostly occurred as single motifs.

The genomes of distant invertebrates, from cnidarians to arthropods, were also found to contain large sets of min-HHRs (fig. 2*D* and supplementary fig. S3, Supplementary Material online), including an example of polydnavirus PLEs integrated within the genome of the *Cotesia congregata* wasp (supplementary fig. S4*A*, Supplementary Material online). Like in trematodes, motifs could be grouped in consensus families, and for each genome, only a few examples mapped within full PLEs. Regarding vertebrates, similar min-HHRs were found within *Xena*, *Poseidon*, and *Neptune* PLEs from diverse fishes (Volff et al. 2001; Dalle Nogare et al. 2002), but also widespread throughout the genomes (fig. 2*B*). Genomes of the coelacanth *Latimeria chalumnae* and the amphibian *Xenopus tropicalis* were remarkable cases, with about 4,000 and 9,000 min-HHRs, respectively. The motifs were classified in several consensus families, and, in a few cases, they were found within the flanking repeats of PLEs (supplementary fig. S4*B* and *C*, Supplementary Material online). Similar motifs were found conserved in different reptiles (turtle

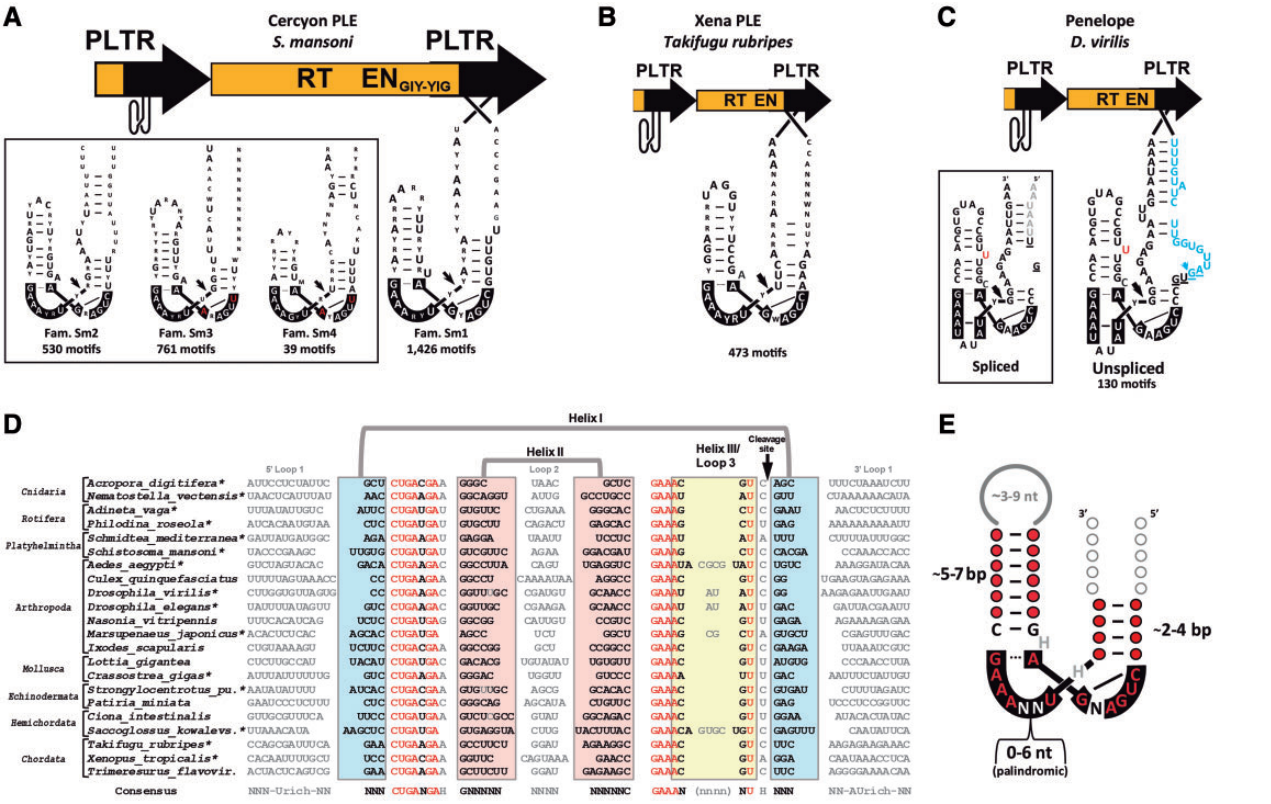

Fig. 2. (*A*) A consensus family of the most frequent min-HHR of *Schistosoma mansoni* PLEs is depicted at their PLTRs. Three other consensus families are shown in the left inset. The less conserved positions (<80%) are depicted with smaller fonts. Exceptional core changes are shown in red. (*B*) Family of min-HHRs found in *Xena* PLEs of the fugu fish. (*C*) min-HHR variant found in *Drosophila virilis* PLEs. The 3′-end of the intron is shown in blue. The predictable HHR resulting after intron splicing is shown in the left inset. (*D*) Structural alignment of representative min-HHRs in metazoans. Conserved nucleotides are shown in red. Helixes I, II, and III are highlighted with colored boxes. Single-stranded nucleotides are shown in gray. HHRs found associated with PLEs are marked with an asterisk, and their accession numbers are shown in supplementary table S1, Supplementary Material online. A larger version of the alignment is shown in supplementary figure S2*A*, Supplementary Material online. (*E*) Consensus motif for the min-HHRs found in metazoan PLEs.

and snakes), whereas analysis of mammalian genomes did not reveal any apparent family of min-HHRs.

Variants of the min-HHRs in Some Metazoan PLEs

Although PLEs were originally discovered in the genome of *Drosophila virilis* (Evgen'ev et al. 1997), our bioinformatic searches did not detect min-HHRs in this organism. After manual inspection of PLEs from *D. virilis*, however, we found an atypical variant of this ribozyme in their PLTRs. This novel motif had specific traits that explain why it had escaped our minimal descriptor, such as the presence of 1) a bulged nucleotide in the middle of Helix II, 2) a canonical-like Helix III with a 2-nt insertion of palindromic sequence, and 3) a shorter (2 bp) Helix I (fig. 2*C*). On the other hand, Helix II was again large (6 bp) and it had the usual bulged base at the 5′-end. Interestingly, the end of the spliceosomal intron described for these PLEs (Arkhipova et al. 2003) mapped with the 5′-end of Helix I, which allows to define a different HHR for the spliced and the unspliced forms (fig. 2*C* and inset). In contrast with the variable min-HHRs described before, the 130 motifs found in *D. virilis* showed a high sequence conservation, with 97 identical HHRs. Similar, although less atypical, HHRs were numerously detected by bioinformatics in PLEs and genome-widespread in *Drosophila* spp. flies (i.e., *D. willistoni*), rotifers (Gladyshev and Arkhipova 2007; Arkhipova et al. 2013), shrimps (Koyama et al. 2013) or mosquitos (AAGE02001300.1), all featured by the presence of a small and palindromic Helix III (fig. 2*D* and supplementary figs. S3 and S5, Supplementary Material online)

HHR Motifs in the Telomere-Associated PLEs from Plants, Fungi, and Protists

EN-deficient PLEs have been reported within telomeric regions of plants, fungi or protist, and postulated as possible antecessors of present-day telomerases (Gladyshev and Arkhipova 2007). Inspection of PLEs from the plant *Selaginella moellendorfii* allowed us to find canonical type-I HHRs in their PLTRs showing typical Helixes I, II, and III, as well as the conserved nucleotides involved in tertiary interactions (fig. 3*A*). PLEs from diverse fungi (fig. 3*B*) and protists (fig. 3*C*), however, showed new type-I HHR variants similar to bacterial motifs (De la Peña and Garcia-Robles 2010b; Jimenez et al. 2011; Perreault et al. 2011), characterized by a large Helix III, whereas Helixes I and II had diverse sizes with no recognizable tertiary interactions between them.

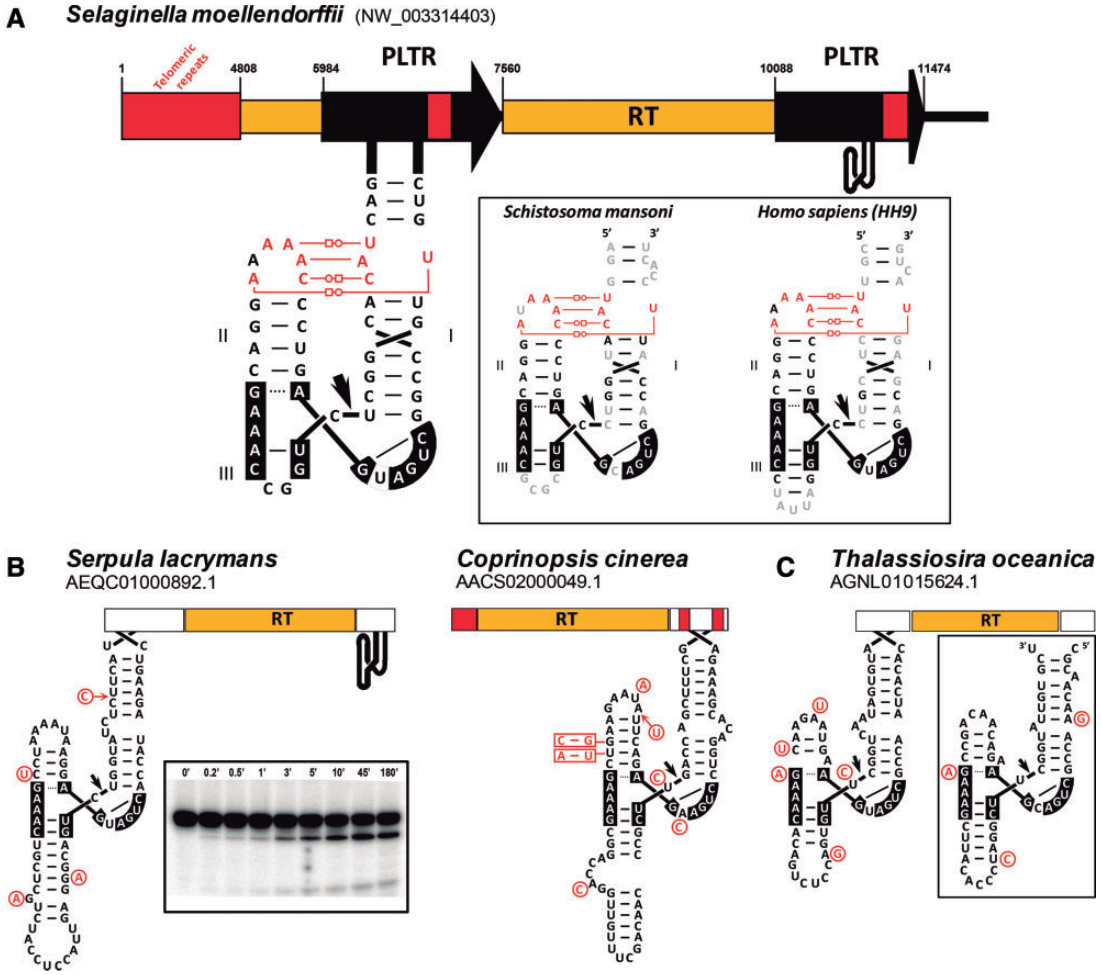

FIG. 3. (*A*) Canonical HHRs found in the PLTRs of PLEs from the plant *Selaginella moellendorffii*. In the right inset, the HHRs found in *Schistosoma mansoni* and humans are shown for comparison, with differences in gray (De la Peña and Garcia-Robles 2010a). (*B*) HHR variants found in retroelements of fungi (inset shows a kinetic analysis of self-cleavage at 1 mM Mg^{2+} of the *Serpula lacrymans* HHR, sequence in black) and (*C*) protists (inset shows a second HHR variant found in the genome of *Thalassiosira oceanica*). Sequence variability is depicted with nucleotides in red.

PLE-HHRs Show Low Self-Cleaving Activity In Vitro

Like most metazoan type-I HHRs, our min-HHRs seem to be selected to work as dimeric motifs. To test their self-cleaving capabilities, a min-HHR from *S. mansoni* was chosen for in vitro analysis. As expected, single motif did not show any detectable self-cleavage activity (data not shown). However, assays with a dimeric and trimeric constructs showed some, though low, cleaving activity (supplementary fig. S6*A*, Supplementary Material online). Self-cleavage was also detected when a Helix III mimicking the dimeric conformation was introduced in a single motif (supplementary fig. S6*B*, Supplementary Material online), but mostly under nonphysiological conditions of Mg^{2+} concentration and far from the cleavage activity reported for canonical ribozymes. Similar results were obtained with an elongated version of the Helix III of *D. virilis* HHR (supplementary fig. S6*C*, Supplementary Material online). On the other hand, the analysis of PLE-HHRs from the *Serpula lacrymans* fungus revealed a more canonical behavior as a single ribozyme, with a k_{obs} of self-cleavage of 1.97 and 0.16 min^{-1} at 10 and 1 mM Mg^{2+}, respectively (fig. 3*B* inset).

Discussion

Our data indicate that novel HHR motifs are preserved in the enigmatic superfamily of PLEs. In the absence of in vivo evidence, a likely role for these motifs would be the self-scission and processing of PLE transposons from precursor RNAs. The low in vitro activity detected for min-HHRs in metazoans suggests that, in vivo, these ribozymes may require host factors (i.e., RNA chaperones or splicing factors) or cofactors to self-cleave more efficiently, although either an intrinsic low activity or functions other than self-cleavage cannot be ruled out. However, the presence of more canonical HHRs in PLEs from protists, plants, and fungi clearly points to an RNA self-cleavage role. Overall, HHRs in eukaryotic PLEs could be mimicking the related group II intron retroelements in bacteria, where a large self-splicing RNA encoding an RT-EN allows the intron to spread throughout the genomes (Lambowitz and Zimmerly 2011).

Of course, the consensus sequence that we obtained for the eukaryotic min-HHRs already contains a bias introduced by our in silico search strategy (i.e., catalytic boxes). However, the retrieved sequences also showed several features not

included in the descriptors that consistently emerged among the obtained solutions, making a random nature for the detected motifs unlikely: 1) Individual genomes show large sets of consensus families full of covariations and compensatory changes, 2) the conserved presence of a nucleotide between positions 9 and 10.1, 3) the highly conserved $G_{10.1}$–$C_{11.1}$ base pair typical of canonical HHRs, and 4) the palindromic nature of positions 15.2–16.2, and loop 3 when present.

One of the most remarkable features of metazoan PLE-HHRs found in this work is their extreme sequence variability for the same motif within every genome, which indicates that these are highly evolving sequences. The sole exception to this high variability was the case of PLE-HHRs of *D. virilis*, whose genome is known to be in the process of ongoing PLE reinvasion (Rozhkov et al. 2013). The high variability for such small motifs would be difficult to explain from a simple mutation-selection process at the DNA level, even considering numerous rounds of PLE invasions. Future studies should explore the possibility of RNA-to-RNA steps for these elements, where much higher mutation rates followed by selection of functional RNA motifs would help to explain these observations.

Taking all these results together, we propose a tentative role for these motifs in the PLEs' replicative mode of transposition, where PLE-HHRs would self-cleave the precursor RNA of the retroelement. Eventually, compatible 5′- and 3′-RNA ends may be ligated to give circular RNAs that could be the template for more-than-unit retrotranscription and genomic insertion through the participation of the RT and EN activities encoded by the retroposon as reported by Pyatkov et al. (2004). Such a possibility would offer a feasible explanation to the typical head-to-tail tandem arrangement described for genomic PLEs, which are known to require more-than-unit copies to become competent for further retrotranspositions (Evgen'ev and Arkhipova 2005) (fig. 1*C*).

In conclusion, our data, together with recent reports describing the presence of HDV ribozymes in non-LTR retrotransposons (Eickbush DG and Eickbush TH 2010; Ruminski et al. 2011), reinforce the idea that small self-cleaving ribozymes are tightly connected with eukariotic retrotransposons. A deeper analysis of current and future genomic data will help us to unveil the secrets enclosed by major constituents of eukaryotic genomes, such as PLEs and retrotransposons in general.

Materials and Methods

Bioinformatic Analysis

Bioinformatic searches in genomic databases were performed through the secondary structure-based software RNAmotif (Macke et al. 2001). The initial descriptor used for min-HHR searches had the stems of Helixes I and II restricted to the canonical 6 and 4 bp found in most HHRs, respectively. Because initial searches with such a descriptor resulted in very low number of hits, more relaxed sizes for stems of Helixes I and II were used (fig. 1*B* and supplementary fig. S7, Supplementary Material online). In this way, the number of motifs found in every genome increased notably, which usually allowed us to define several groups or consensus families of min-HHRs at the sequence level, and a smaller fraction of motifs that could not be grouped in any family and were discarded for further analysis. Loop 1 and the closing stems of Helix I were not considered in the descriptor. Thus, for each case, this possibility was manually analyzed and depicted. In theory, the aim of the min-HHR motif would be to work under a dimeric conformation, and accordingly, the obtained hits were filtered in order to find them as tandem repeats and/or in close proximity (below 50 kb). The data obtained through secondary structure-based searches were combined and extended with sequence homology analysis against related genomes (BLAST/BLAT). Sequence alignments were done with ClustalX (Larkin et al. 2007). Consensus sequences for each HHR family were obtained through WebLogo3 software (Crooks et al. 2004).

In Vitro Transcription

DNA constructs of the *cis*-acting HHRs carrying the T7 promoter were obtained synthetically by recursive polymerase chain reactions with partially overlapping primers (IDT Technologies Inc.) carrying the sequence of the HHR of interest. Obtained products were cloned in pUC18 plasmid opened with *Sma*I/*Xba*I enzymes. RNAs were synthesized by in vitro transcription of *Xba*I-linearized plasmids containing the corresponding inserts. Transcription reactions contained: 40 mM Tris–HCl, pH 8, 6 mM $MgCl_2$, 2 mM spermidine, 0.5 mg/ml RNase-free bovine serum albumin, 0.1% Triton X-100, 10 mM dithiothreitol, 1 mM each of ATP, CTP and GTP, 0.1 mM UTP plus 0.5 μCi/μl [α-32P]UTP, 2 U/μl of human placental ribonuclease inhibitor, 20 ng/μl of plasmid DNA, and 4 U/μl of T7 RNA polymerase. After incubation at 37 °C for 1–2 h, products were fractionated by polyacrylamide gel electrophoresis (PAGE) in 15% gels with 8 M urea. The uncleaved primary transcripts, which represented the major fraction of the transcribed RNAs (from ~85% to 98%), were eluted by crushing the gel pieces and extracting them with phenol saturated with buffer (Tris–HCl 10 mM, pH 7.5, ethylenediaminetetraacetic acid [EDTA] 1 mM, sodium dodecyl sulfate 0.1%), recovered by ethanol precipitation, and resuspended in deionized and sterile water.

Self-Cleavage Kinetics under Protein-Free Conditions

To determine the cleaving rate constants, uncleaved primary transcripts (from 1 nM to 1 μM) were incubated in 20 μl of 50 mM Tris–HCl, pH 7.5 for 1 min at 95 °C and slowly cooled to 25 °C for 15 min. After taking a zero-time aliquot, self-cleavage reactions were triggered by adding $MgCl_2$ at a final concentration of 1–50 mM. Aliquots were removed at the appropriate time intervals and quenched with a 5-fold excess of stop solution (8 M urea, 50% formamide, 50 mM EDTA, 0.1% xylene cyanol and bromophenol blue) at 0 °C. Substrates and cleavage products were separated by PAGE in 15% denaturing gels. The product fraction at different times, F_t, was determined by quantitative scanning of the corresponding gel bands and fitted to the equation $F_t = F_0 + F_\infty(1 - e^{-kt})$, where F_0 and F_∞ are the product

fractions at zero time and at the reaction endpoint, respectively, and k is the first order rate constant of cleavage (k_{obs}).

Database Accession Numbers of PLE-HHRs

Supplementary table S1, Supplementary Material online, shows the GenBank accession numbers of the HHR sequences of figure 2*D* and supplementary figure S3, Supplementary Material online, that were found associated with PLE ORFs.

Supplementary Material

Supplementary figures S1–S7 and table S1 are available at *Molecular Biology and Evolution* online (http://www.mbe.oxfordjournals.org/).

Acknowledgments

This work was supported by the Ministerio de Economia y Competitividad (grant number BFU2011-23398).

References

Arkhipova IR, Pyatkov KI, Meselson M, Evgen'ev MB. 2003. Retroelements containing introns in diverse invertebrate taxa. *Nat Genet.* 33:123–124.

Arkhipova IR, Yushenova IA, Rodriguez F. 2013. Endonuclease-containing *Penelope* retrotransposons in the bdelloid rotifer *Adineta vaga* exhibit unusual structural features and play a role in expansion of host gene families. *Mob DNA.* 4:19.

Berriman M, Haas BJ, LoVerde PT, Wilson RA, Dillon GP, Cerqueira GC, Mashiyama ST, Al-Lazikani B, Andrade LF, Ashton PD, et al. 2009. The genome of the blood fluke *Schistosoma mansoni*. *Nature* 460: 352–358.

Crooks GE, Hon G, Chandonia JM, Brenner SE. 2004. WebLogo: a sequence logo generator. *Genome Res.* 14:1188–1190.

Dalle Nogare DE, Clark MS, Elgar G, Frame IG, Poulter RT. 2002. Xena, a full-length basal retroelement from tetraodontid fish. *Mol Biol Evol.* 19:247–255.

Daros JA, Flores R. 1995. Identification of a retroviroid-like element from plants. *Proc Natl Acad Sci U S A.* 92:6856–6860.

De la Peña M, Flores R. 2001. An extra nucleotide in the consensus catalytic core of a viroid hammerhead ribozyme: implications for the design of more efficient ribozymes. *J Biol Chem.* 276: 34586–34593.

De la Peña M, Gago S, Flores R. 2003. Peripheral regions of natural hammerhead ribozymes greatly increase their self-cleavage activity. *EMBO J.* 22:5561–5570.

De la Peña M, Garcia-Robles I. 2010a. Intronic hammerhead ribozymes are ultraconserved in the human genome. *EMBO Rep.* 11:711–716.

De la Peña M, Garcia-Robles I. 2010b. Ubiquitous presence of the hammerhead ribozyme motif along the tree of life. *RNA* 16: 1943–1950.

Eickbush DG, Eickbush TH. 2010. R2 retrotransposons encode a self-cleaving ribozyme for processing from an rRNA cotranscript. *Mol Cell Biol.* 30:3142–3150.

Epstein LM, Gall JG. 1987. Self-cleaving transcripts of satellite DNA from the newt. *Cell* 48:535–543.

Evgen'ev MB, Arkhipova IR. 2005. *Penelope*-like elements—a new class of retroelements: distribution, function and possible evolutionary significance. *Cytogenet Genome Res.* 110:510–521.

Evgen'ev MB, Zelentsova H, Shostak N, Kozitsina M, Barskyi V, Lankenau DH, Corces VG. 1997. *Penelope*, a new family of transposable elements and its possible role in hybrid dysgenesis in *Drosophila virilis*. *Proc Natl Acad Sci U S A.* 94:196–201.

Ferbeyre G, Smith JM, Cedergren R. 1998. Schistosome satellite DNA encodes active hammerhead ribozymes. *Mol Cell Biol.* 18:3880–3888.

Ferre-D'Amare AR, Scott WG. 2010. Small self-cleaving ribozymes. *Cold Spring Harb Perspect Biol.* 2:a003574.

Flores R, Delgado S, Gas ME, Carbonell A, Molina D, Gago S, de la Peña M. 2004. Viroids: the minimal non-coding RNAs with autonomous replication. *FEBS Lett.* 567:42–48.

Forster AC, Davies C, Sheldon CC, Jeffries AC, Symons RH. 1988. Self-cleaving viroid and newt RNAs may only be active as dimers. *Nature* 334:265–267.

Gilbert W. 1986. The RNA world. *Nature* 319:618.

Gladyshev EA, Arkhipova IR. 2007. Telomere-associated endonuclease-deficient *Penelope*-like retroelements in diverse eukaryotes. *Proc Natl Acad Sci U S A.* 104:9352–9357.

Hammann C, Luptak A, Perreault J, de la Peña M. 2012. The ubiquitous hammerhead ribozyme. *RNA* 18:871–885.

Hertel KJ, Pardi A, Uhlenbeck OC, Koizumi M, Ohtsuka E, Uesugi S, Cedergren R, Eckstein F, Gerlach WL, Hodgson R, et al. 1992. Numbering system for the hammerhead. *Nucleic Acids Res.* 20:3252.

Hutchins CJ, Rathjen PD, Forster AC, Symons RH. 1986. Self-cleavage of plus and minus RNA transcripts of avocado sunblotch viroid. *Nucleic Acids Res.* 14:3627–3640.

Jimenez RM, Delwart E, Luptak A. 2011. Structure-based search reveals hammerhead ribozymes in the human microbiome. *J Biol Chem.* 286:7737–7743.

Khvorova A, Lescoute A, Westhof E, Jayasena SD. 2003. Sequence elements outside the hammerhead ribozyme catalytic core enable intracellular activity. *Nat Struct Biol.* 10:708–712.

Koyama T, Kondo H, Aoki T, Hirono I. 2013. Identification of two *Penelope*-like elements with different structures and chromosome localization in kuruma shrimp genome. *Mar Biotechnol.* 15: 115–123.

Kruger K, Grabowski PJ, Zaug AJ, Sands J, Gottschling DE, Cech TR. 1982. Self-splicing RNA: autoexcision and autocyclization of the ribosomal RNA intervening sequence of *Tetrahymena*. *Cell* 31: 147–157.

Lambowitz AM, Zimmerly S. 2011. Group II introns: mobile ribozymes that invade DNA. *Cold Spring Harb Perspect Biol.* 3: a003616.

Larkin MA, Blackshields G, Brown NP, Chenna R, McGettigan PA, McWilliam H, Valentin F, Wallace IM, Wilm A, Lopez R, et al. 2007. Clustal W and Clustal X version 2.0. *Bioinformatics* 23: 2947–2948.

Macke TJ, Ecker DJ, Gutell RR, Gautheret D, Case DA, Sampath R. 2001. RNAMotif, an RNA secondary structure definition and search algorithm. *Nucleic Acids Res.* 29:4724–4735.

Martick M, Horan LH, Noller HF, Scott WG. 2008. A discontinuous hammerhead ribozyme embedded in a mammalian messenger RNA. *Nature* 454:899–902.

Martick M, Scott WG. 2006. Tertiary contacts distant from the active site prime a ribozyme for catalysis. *Cell* 126:309–320.

Perreault J, Weinberg Z, Roth A, Popescu O, Chartrand P, Ferbeyre G, Breaker RR. 2011. Identification of hammerhead ribozymes in all domains of life reveals novel structural variations. *PLoS Comput Biol.* 7:e1002031.

Prody GA, Bakos JT, Buzayan JM, Schneider IR, Bruening G. 1986. Autolytic processing of dimeric plant virus satellite RNA. *Science* 231:1577–1580.

Przybilski R, Graf S, Lescoute A, Nellen W, Westhof E, Steger G, Hammann C. 2005. Functional hammerhead ribozymes naturally encoded in the genome of *Arabidopsis thaliana*. *Plant Cell* 17: 1877–1885.

Pyatkov KI, Arkhipova IR, Malkova NV, Finnegan DJ, Evgen'ev MB. 2004. Reverse transcriptase and endonuclease activities encoded by *Penelope*-like retroelements. *Proc Natl Acad Sci U S A.* 101: 14719–14724.

Rojas AA, Vazquez-Tello A, Ferbeyre G, Venanzetti F, Bachmann L, Paquin B, Sbordoni V, Cedergren R. 2000. Hammerhead-mediated processing of satellite pDo500 family transcripts from *Dolichopoda* cave crickets. *Nucleic Acids Res.* 28:4037–4043.

Roth A, Weinberg Z, Chen AG, Kim PB, Ames TD, Breaker RR. 2014. A widespread self-cleaving ribozyme class is revealed by bioinformatics. *Nat Chem Biol.* 10:56–60.

Rozhkov NV, Schostak NG, Zelentsova ES, Yushenova IA, Zatsepina OG, Evgen'ev MB. 2013. Evolution and dynamics of small RNA response to a retroelement invasion in *Drosophila*. *Mol Biol Evol*. 30: 397–408.

Ruminski DJ, Webb CH, Riccitelli NJ, Luptak A. 2011. Processing and translation initiation of non-LTR retrotransposons by hepatitis delta virus (HDV)-like self-cleaving ribozymes. *J Biol Chem*. 286: 41286–41295.

Seehafer C, Kalweit A, Steger G, Gräf S, Hammann C. 2011. From alpaca to zebrafish: hammerhead ribozymes wherever you look. *RNA* 17: 21–26.

Symons RH. 1997. Plant pathogenic RNAs and RNA catalysis. *Nucleic Acids Res*. 25:2683–2689.

Volff JN, Hornung U, Schartl M. 2001. Fish retroposons related to the *Penelope* element of *Drosophila virilis* define a new group of retrotransposable elements. *Mol Genet Genomics*. 265:711–720.